WARWICK
THE UNIVERSITY OF WARWICK

Manuscript version: Author's Accepted Manuscript
The version presented in WRAP is the author's accepted manuscript and may differ from the published version or Version of Record.

Persistent WRAP URL:
http://wrap.warwick.ac.uk/163773

How to cite:
Please refer to published version for the most recent bibliographic citation information. If a published version is known of, the repository item page linked to above, will contain details on accessing it.

Copyright and reuse:
The Warwick Research Archive Portal (WRAP) makes this work by researchers of the University of Warwick available open access under the following conditions.

Copyright © and all moral rights to the version of the paper presented here belong to the individual author(s) and/or other copyright owners. To the extent reasonable and practicable the material made available in WRAP has been checked for eligibility before being made available.

Copies of full items can be used for personal research or study, educational, or not-for-profit purposes without prior permission or charge. Provided that the authors, title and full bibliographic details are credited, a hyperlink and/or URL is given for the original metadata page and the content is not changed in any way.

Publisher's statement:
Please refer to the repository item page, publisher's statement section, for further information.

For more information, please contact the WRAP Team at: wrap@warwick.ac.uk.

warwick.ac.uk/lib-publications

Proceedings of the ASME 2021
48th Annual Review of Progress in
Quantitative Nondestructive Evaluation
QNDE2021
July 28-30, 2021, Virtual, Online

QNDE2021-74942

DETECTION OF DEFECTS IN TITANIUM USING SHEAR HORIZONTAL GUIDED WAVES

Christian Peyton[1,2], Rachel S. Edwards[1], Steve Dixon[1], Ben Dutton[2], Wilson Vesga[2]

[1]Department of Physics, University of Warwick, Coventry, UK
[2]Manufacturing Technology Centre, Coventry, UK

ABSTRACT

This paper investigates the interaction behaviour between the fundamental shear horizontal guided wave mode and small defects, in order to understand and develop an improved inspection system for titanium samples. In this work, an extensive range of defect sizes have been simulated using finite element software. The SH0 reflection from a defect has been shown previously to depend on its length as the total reflection consists of reflections from both the front and back face. However, for small defect widths, this work has found that the width also affects this interference, changing the length at which the reflection is largest. In addition, the paper looks at how the size of the defect affects the mode converted S0 reflection and SH0 diffraction. The relationship between the SH0 diffraction and defect size is shown to be more complex compared to the reflections. The mode converted S0 reflection occurs at an angle to the incident wave direction; therefore, the most suitable angle for the detection has been found. Simultaneous measurement of multiple waves would bring benefits to inspection.

Keywords: Shear horizontal (SH) waves; reflection behaviour, S0 mode conversion.

1. INTRODUCTION

Inspection of defects in welds is challenging but of great interest to industry. Having the most effective inspection setup allows for greater potential in detecting critical flaws. An improved inspection approach can be achieved by understanding the interaction between the fundamental shear horizontal guided wave mode (SH0) and defects of different sizes [1]. This understanding will result in the selection of suitable wavelengths and methods of inspection, enabling the detection of flaws of the required dimension. The motivation for understanding this behaviour is to develop a system capable of live inspections of laser welds in thin titanium samples. Titanium is traditionally a difficult sample to inspect; its larger grain structure results in low signal-to-noise ratio (SNR) for ultrasonic inspection and reduced repeatability [2], [3].

Research has been performed previously on how to detect small defects with guided waves, using different guided wave mode types and forms of transduction [4]–[6]. The work in this paper focuses on the SH0 reflection and diffraction from defects of different sizes. In addition, the mode converted Lamb wave, S0, from the defect has also been studied, looking at its dependence on defect dimensions and the potential for a combined inspection approach. All of the work reported here was performed using finite element simulations.

1.1 Shear Horizontal Guided Waves

The behaviour of shear horizontal (SH) waves is described by the dispersion curves. Figure 1 shows the phase velocity dispersion curve for a 1 mm thick titanium plate. The SH waves are affected by the bulk shear speed of the component, the thickness of the sample and the operating frequency. Depending on these conditions, there are an infinite number of symmetric and anti-symmetric SH waves that can exist [7]. Alongside the dispersion curve for the group velocity, these show the mode velocities for a specific frequency thickness product. This work has focused on the zeroth mode (SH0), which has a number of beneficial properties. The main benefit is that it is non-dispersive; this means that both the group and phase velocities are equal and do not change with frequency. SH0 waves can be used for the inspection of welds [1], as well as thickness inspections when used in parallel with higher order SH waves [8].

This work used a 6 mm wavelength for the SH0 wave mode, determined by the generation transducer geometry. To generate this wavelength in a 1mm thick titanium sample, a driving frequency of 516.67 kHz is used. It can be seen that there are no other SH wave modes present at this frequency thickness product, because all higher order SH wave modes have cutoff frequencies that are greater than this. For example, the cutoff for the next mode (SH1) is 1550 kHz [7].

1.2 SH0 Defect Interaction

There have been previous studies on the interaction between SH0 waves and defects. The reflection behaviour between the SH0 mode and a notch is dependent on interference between the reflections from the front and back faces [9]–[12]. Demma et al.

© 2019 by ASME

showed that a notch could be represented as two thickness changes; a step down from the plate thickness to the notch depth followed by a step up from notch depth to plate thickness [9]. In a simple model, the separation between these thickness changes alters the overall reflection magnitude from the notch. The separation is considered as the ratio between defect length (physical separation, L) and SH0 wavelength λ, i.e. L/λ, resulting in a maximum reflection magnitude being present at;

$$\frac{L}{\lambda} = \frac{n\,\lambda}{2} + \frac{\lambda}{4}, \quad (1)$$

and a minimum at;

$$\frac{L}{\lambda} = \frac{n\,\lambda}{2}, \quad (2)$$

where n is an integer. However, this simple model does not account for phase changes that occur at the thickness steps. When this is considered, the maxima and minima positions shift to the left, lowering their L/λ values, but the oscillating behaviour of maxima and minima reflection magnitudes is still present [9]. This dependence on notch length is only seen in the low-frequency SH regime, where the frequency is less than the SH1 mode cut off. The sensitivity to the defect length is reduced for higher-order guided wave modes [10].

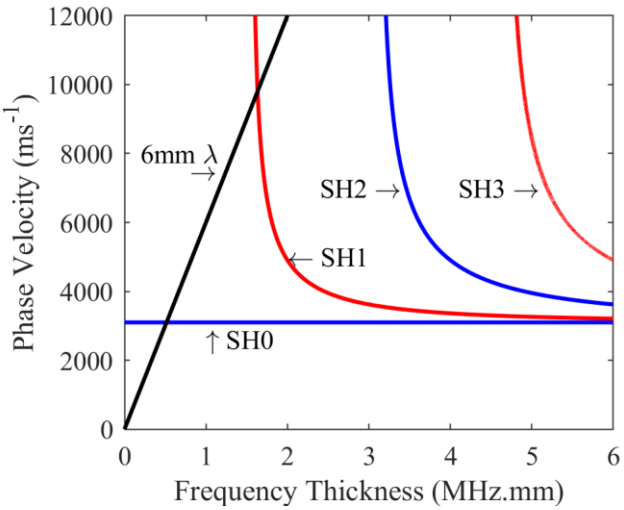

FIGURE 1: PHASE VELOCITY DISPERSION CURVE FOR SHEAR HORIZONTAL GUIDED WAVES IN 1 mm THICK TITANIUM PLATE.

Defects that are antisymmetric through the plate thickness, such as surface-breaking notches, allow for symmetric and antisymmetric mode reflections, while symmetric defects through the plate thickness only allow for the reflection of symmetric wave modes [13], [14]. The notches in this work are all antisymmetric through the plate thickness, but as we are below the cutoff for higher order SH guided wave modes, the only SH mode present in the far field reflection is SH0 [13].

The reflection behaviour for more complex elliptical shape defects has also been studied. The relationship between the defect length and wavelength is still present; however, as the angle of incidence changes, so does the defect's effective length. Therefore, the magnitude of the reflection is also affected [11]. For imaging of more complex and realistic shape defects with SH guided waves, performing multiple angle incidence inspections will provide greater information on the defect shape.

Further work performed by Ratassepp et al. and Rajagopal et al. investigated the effect when a crack is orientated parallel or perpendicular to the SH0 propagation direction, respectively [12], [15]. They found the generation of surface waves propagating along the discontinuities (free surfaces) and the diffraction occurring at the crack tips to be key factors affecting the reflection behaviour. The diffraction behaviour also depends on the interference of waves from the multiple locations around the defect where diffraction could occur. The primary sources are at the crack tip, and from the surface wave diffracting at the end of the crack. It would be possible to improve the guided wave imaging of defects by using both the reflection and diffraction behaviour. However, further work into understating the propagation along the notch face is required [12].

2. METHODOLOGY

The defect length, which is referred to in this paper, is the dimension of the defect in the direction parallel to the SH0 wave propagation (X-direction in Figure 2). The width is the dimension perpendicular to this but parallel to the plate surface (Y-direction), and finally, the depth is the through thickness dimension of the defect (Z-direction).

Finite element analysis has been on performed a 1 mm thick titanium sheet using PZFlex finite element software. The material properties used in the simulation were the density and shear wave speed; these were set to 4480 kg m^{-3} and 3100 m s^{-1}, respectively. The simulation was performed on a plate of dimensions 300 × 200 × 1 mm, with the SH0 wave propagating along in the X-direction and its oscillation in the Y-direction. To remove unwanted reflections, the extremal X and Y surfaces were set to absorbing boundary conditions. This removes the reflection from the ends and edges of the plate. The top and bottom surfaces were kept as free boundaries to allow for the generation of the SH wave and propagation of mode-converted waves.

The centre of the wave generation was positioned at x = 0, the plate edges were $x_{min} = -50$ mm and $x_{max} = 250$ mm. The front face of the defect was positioned at $x = 100$ mm, fixed along the centre-line in the Y-direction, as shown in Figure 2. A range of different defect sizes have been simulated, as well as simulations with no defect present. The simulations have been run with cubic elements, 0.1 mm in size, allowing for a total of 10 elements through the thickness of the plate.

Generation of the SH wave was performed by a spatial force profile, f, that imitates the forces induced by a periodic permanent magnet array (PPM) EMAT. The force was applied to nodes on the top surface of the plate.

$$f[i] = \sin\left(\frac{2\pi x[i]}{\lambda}\right), \quad (3)$$

© 2019 by ASME

where $x[i]$ represents the position of the node in the X-direction, the force is applied in the Y-direction, for *N* periods in the PPM EMAT. The number of periods was set to three, to match the physical size of the PPM EMATs available for testing. To implement this in 3D simulations rather than 2D [16], the width of the PPM EMAT also needs to be represented. This has been set by applying the width of the active area for the spatial force profile as $Y_{centreline} \pm \lambda$. This approximately matches the size of the EMATs used experimentally.

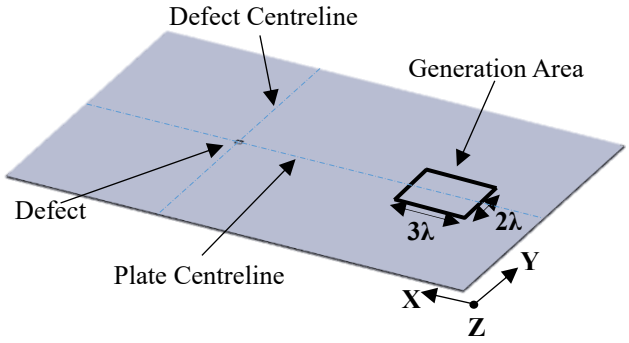

FIGURE 2: SIMULATION SETUP SCHEMATIC.

A driving frequency of 516.67 kHz was used to generate an SH0 mode with a wavelength of 6 mm. The input was a 3 cycle tone burst. For the reflection behaviour results, data was recorded every millimetre along the centre-line. A total of 70 different notch sizes were simulated to provide detailed insight into the relationship between notch size and SH0 reflection. However, the notch depth was kept at 0.5 mm throughout.

Measuring positions and velocity component varied depending on the wave mode which was being considered. The SH0 reflection was detected by measuring the Y-velocity, with the reflection magnitude analysed at 70 mm from the defect's front face for all defects. The SH0 diffraction was measured along the defect centreline 75 mm from the defect edge; the X-velocity was used for this wave mode. The S0 wave mode was detected using both the X and Y velocities.

3. RESULTS AND DISCUSSION

3.1 SH0 Reflection

Initial investigations were performed to see if the 6 mm wavelength was suitable for detecting defect sizes significantly smaller than the wavelength. Simulations were performed with defects of different sizes and for a blank plate for comparison. The time traces from these were then compared, as well as their respective spectrograms, with examples shown in Figure 3.

The time traces show the direct incident wave passing the measuring position at around 10 µs, followed by some high-frequency noise. The defect simulations then show an additional wavepacket at the expected arrival time of the SH0 wave. This additional wavepacket can be clearly seen in the spectrograms, where the frequency content matches that of the incident SH0 wave. The arrival time also matches the predicted arrival time of a defect reflection. It was also found that the high-frequency component present between the incident and reflected signals dispersed very quickly and cannot be seen after 50 mm of travel, well before any interaction with the defect. From this, there was confidence that this wavelength and wave mode was suitable for inspecting smaller defects, and therefore appropriate for this investigation.

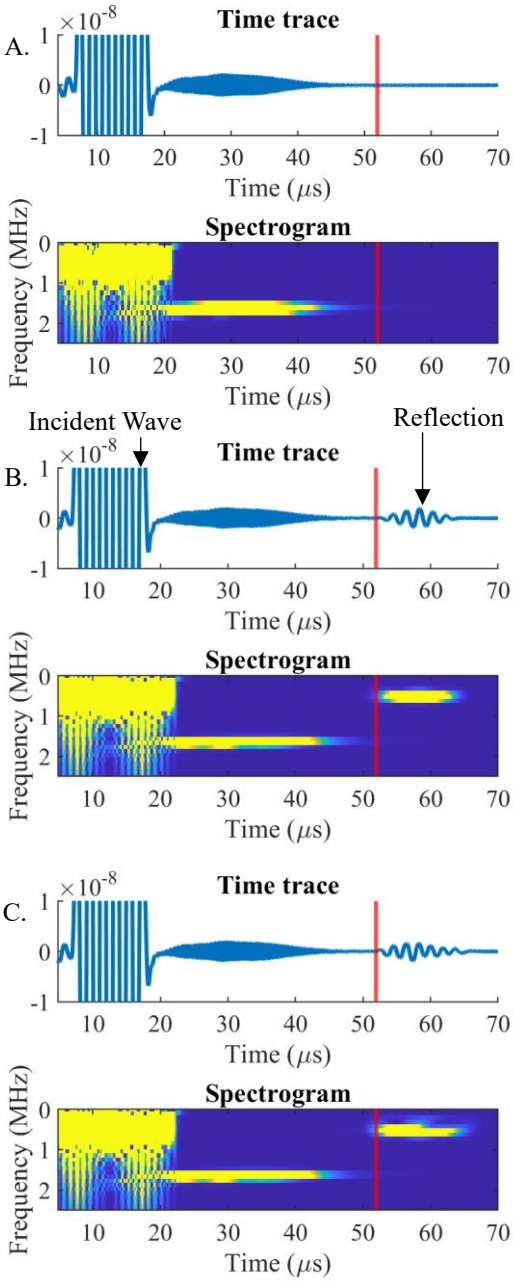

FIGURE 3: TIME TRACES AND SPECTROGRAMS FROM DIFFERENT DEFECT SIZE SIMULATIONS. A) BLANK SAMPLE. B) DEFECT SIZE 1*1*0.5 mm. C) DEFECT SIZE 3*3*0.5 mm. VERTICAL RED LINE INDICATES EXPECTED ARRIVAL OF SH0 REFLECTION.

To understand how the defect size affects the SH0 reflection magnitude, a method of comparing the reflections was required. This was done through the use of a reflection coefficient (RC)

© 2019 by ASME

defined in equation (4). The RC is the ratio between the peak-to-peak amplitude (pk2pk) of the reflected signal and the peak-to-peak amplitude of a direct signal, where the direct and reflected signals have travelled equal distances;

$$RC = \frac{Peak - to - peak\ reflection\ amplitude}{Peak - to - peak\ direct\ amplitude}. \quad (4)$$

The reflection coefficients can be seen in the surface plot in Figure 4. This shows that for defects with a fixed length, increasing the width results in an increase in the reflection coefficient. For a fixed defect width, increasing the defect length results in a maximum somewhere between 1 and 1.5 mm. This fits in with the literature, which stated maxima are expected at a L/λ value of below 0.25, which for a 6 mm wavelength is at L = 1.5 mm. However, previous work has not considered the effect of width on this position. A 4th order polynomial fit was applied to the reflection coefficient values for each fixed width, with the fits shown in Figure 5. This allowed for more accurate maxima positions to be calculated.

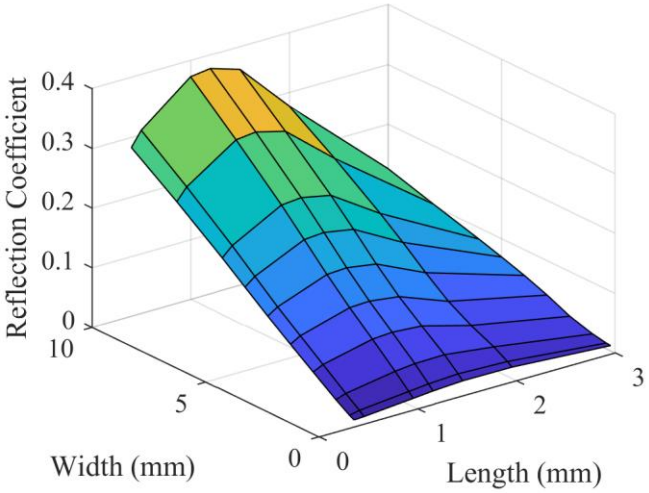

FIGURE 4: SURFACE PLOT SHOWING REFLECTION COEFFICIENT VALUES FOR DIFFERENT DEFECT SIZES.

The fits to the simulated data show that the L/λ value at which the peak reflection coefficient occurs is stable for widths greater than 3 mm. However, for widths less than this, the defect length at which the reflection coefficient is greatest increases. This suggests that the defect width influences the interference of the two reflected signals. The narrower the defect, the longer the length for maximum reflection magnitude.

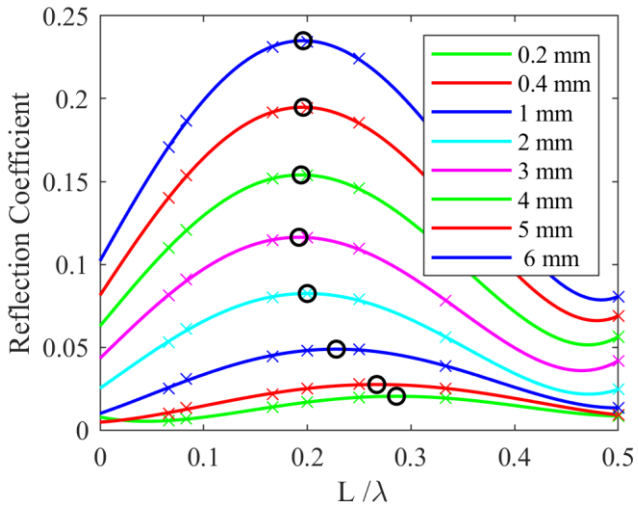

Figure 5: POLYNOMIAL FIT AND MAXIMA REFLECTION COEFFICIENT FOR EACH DEFECT WIDTH.

3.2 S0 Reflection

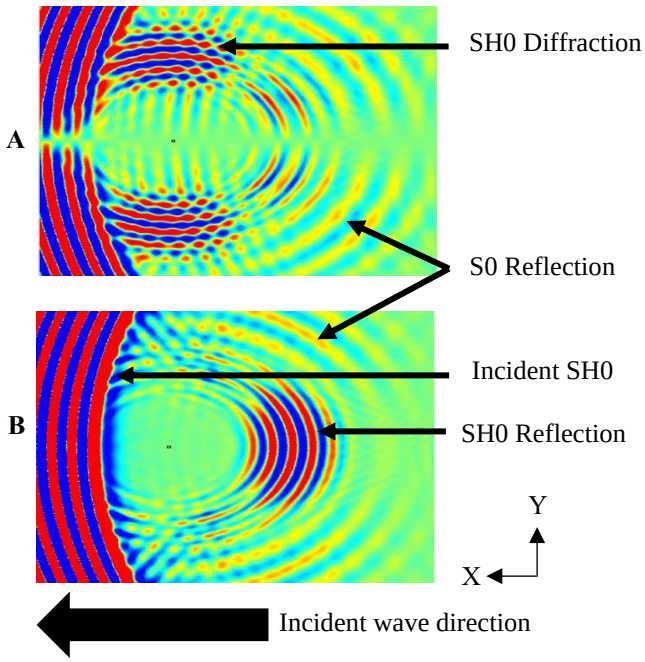

Figure 6: SIMULATION COLOUR MAP AFTER INCIDENT SH0 HAS INTERACTED WITH A DEFECT. DEFECT SIZED 3*1*0.5 mm. A) X-VELOCITY. B) Y-VELOCITY.

When the SH0 mode interacts with a defect, additional modes are generated and transmitted. One of these modes is the S0 Lamb guided wave; the behaviour of this wave was found by inspecting the different velocity directions' colourmaps generated from the simulations, with examples shown in Figure 6. These show a reflection from the defect at an angle from the centreline. A range of time traces were then compared at multiple angles, and it was found that this wavepacket arrival matches a wave with a velocity similar to the expected value for an S0

© 2019 by ASME

mode at this frequency. The S0 wave mode can be seen in both X and Y velocity maps due to the in-plane displacement of the S0 mode dominating and its propagation direction.

The angle at which the S0 had the greatest reflection was investigated, for a defect sized 1*4*0.5 mm. The in-plane motion of the S0 mode is in both the X and Y velocities, and both must be measured and combined to gain an accurate representation of the magnitude of the mode-converted wave. The amplitudes of the peak-to-peak values in the S0 arrival window at different angles for the X and Y velocities were measured. Then the S0 peak-to-peak amplitude was calculated using trigonometry at each angle. Figure 7 shows this and the contributing X and Y velocity peak-to-peak amplitudes. The angle with the greatest peak-to-peak was at 50 degrees; this is measured relative to the Y-direction centreline, Figure 2.

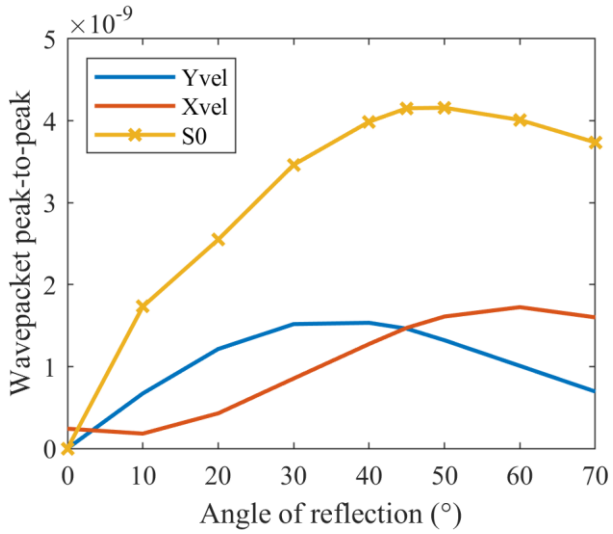

Figure 7: S0 MODE REFLECTION MAGNITUDES AT DIFFERENT ANGLES.

3.3 SH0 Diffraction

The simulation colourmap, Figure 6, also showed the existence of an SH0 diffraction at 90 degrees to the incident wave propagation direction in the X velocity data. To confirm that this was the diffracted SH0 mode, the time traces and spectrograms from a blank plate and the defect simulations were compared, with the data shown in Figure 8. The blank time trace shows no signal at the expected time (shown by a red line), whereas both defect samples show a clear wavepacket at the expected arrival time. The spectrogram confirms that this wavepacket has the expected frequency. The two wavepackets that are present in the blank sample, and before the diffracted SH0 signal in the defect samples, correspond to the direct S0 and SH0 modes which are generated.

Figure 9 summarises how the different defect sizes affect the magnitude of the SH0 diffraction. It is known from literature that the crack length at which maximum diffraction occurs is approximately 0.6 to 0.7 L/λ [12], [15]. However, for notch-like defects, as used in this work, the behaviour is more complex. Increasing the defect width results in a significant change in the L/λ peak position. Also, for each length, larger widths do not result in greater diffraction magnitudes. Therefore, the diffraction magnitude is highly sensitive to both the length and width of the defect.

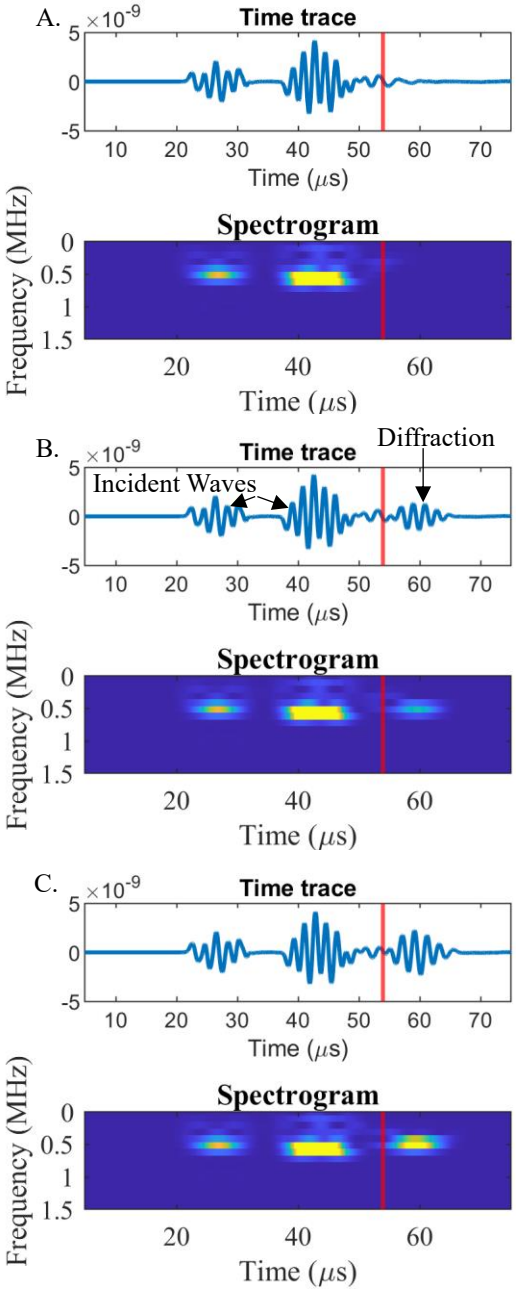

Figure 8: TIMES TRACES AND SPECTROGRAMS FOR SH0 DIFFRACTION. A) BLANK SAMPLE. B) DEFECT SIZE 1*1*0.5 mm. C) DEFECT SIZE 3*3*0.5 mm. VERTICAL RED LINE INDICATES EXPECTED ARRIVAL OF SH0 DIFFRACTION

© 2019 by ASME

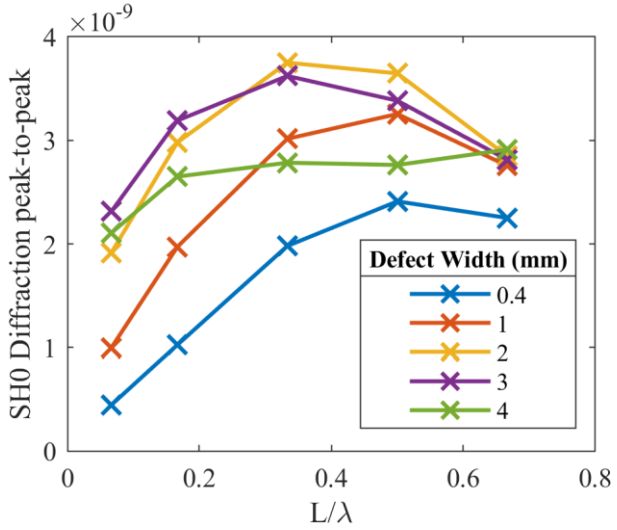

Figure 9: DIFFRACTED SH0 SIGNAL PEAK-TO-PEAK.

4. CONCLUSION

Finite element analysis has been performed to help understand the interaction between shear horizontal guided waves and small defects. Understanding this relationship allows for an appropriate wavelength to be used, giving the greatest probability of detection. Initially, the behaviour of the SH0 reflection from a defect was studied. This found that the defect width affects the length at which maximum reflection occurs. The behaviour was identified for small defects with widths less than 2 mm when a 6 mm wavelength is used.

Alongside the SH0 reflection, there is also a mode converted S0 reflection and an SH0 diffracted signal transmitted from the defect. The S0 is reflected from the defect at an angle. The angle with maximum reflection was found to be 50°. The SH0 diffraction was also detected successfully for a large range of defects. However, the relationship between diffraction magnitude and defect size is much more complex than the reflections, due to the additional sources of diffraction.

Work is in progress to experimentally verify these findings. Electromagnetic acoustic transducers are being used to replicate the simulations as they are efficient generators of shear horizontal waves. Results are thus far in good agreement with the predictions from modelling, and will be detailed in a separate publication. Future work will consider the optimal detection modality; which wave modes are suitable for analysis, and how the reflection, diffraction, and mode converted waves could be used in conjunction to give a high probability of detection for the small defects which can be present in welds.

ACKNOWLEDGEMENTS

The author would like to thank the UK research centre for non-destructive evaluation (RCNDE), the University of Warwick and the Manufacturing Technology Centre.

REFERENCES

[1] P. A. Petcher and S. Dixon, “Weld defect detection using PPM EMAT generated shear horizontal ultrasound,” *NDT E Int.*, vol. 74, pp. 58–65, 2015, doi: 10.1016/j.ndteint.2015.05.005.

[2] E. Escobar-Ruiz, D. C. Wright, I. J. Collison, P. Cawley, and P. B. Nagy, “Reflection Phase Measurements for Ultrasonic NDE of Titanium Diffusion Bonds,” *J. Nondestruct. Eval.*, vol. 33, no. 4, pp. 535–546, 2014, doi: 10.1007/s10921-014-0250-z.

[3] H. V. Patel, S. Woods, X. Jian, I. Cooper, T. Chady, and S. Michau, “A new and novel inspection system for titanium billets,” in *Non-Destructive Testing Conference 2010, NDT 2010*, 2010, pp. 94–103.

[4] C. B. Thring, Y. Fan, and R. S. Edwards, “Multi-coil focused EMAT for characterisation of surface-breaking defects of arbitrary orientation,” *NDT E Int.*, vol. 88, no. February, pp. 1–7, 2017, doi: 10.1016/j.ndteint.2017.02.005.

[5] O. Trushkevych and R. S. Edwards, “Characterisation of small defects using miniaturised EMAT system,” *NDT E Int.*, vol. 107, no. May, p. 102140, 2019, doi: 10.1016/j.ndteint.2019.102140.

[6] L. Yang and I. C. Ume, “Inspection of notch depths in thin structures using transmission coefficients of laser-generated Lamb waves,” *Ultrasonics*, vol. 63, pp. 168–173, Dec. 2015, doi: 10.1016/J.ULTRAS.2015.07.004.

[7] J. L. Rose, *Ultrasonic Guided Waves in Solid Media*. Cambridge University Press, 2014.

[8] S. Dixon, P. A. Petcher, Y. Fan, D. Maisey, and P. Nickolds, “Ultrasonic metal sheet thickness measurement without prior wave speed calibration,” *J. Phys. D. Appl. Phys.*, vol. 46, no. 44, 2013, doi: 10.1088/0022-3727/46/44/445502.

[9] A. Demma, P. Cawley, and M. Lowe, “Scattering of the fundamental shear horizontal mode from steps and notches in plates,” *J. Acoust. Soc. Am.*, vol. 113, no. 4, pp. 1880–1891, 2003, doi: 10.1121/1.1554694.

[10] A. Pau, D. V. Achillopoulou, and F. Vestroni, “Scattering of guided shear waves in plates with discontinuities,” *NDT E Int.*, vol. 84, pp. 67–75, 2016, doi: 10.1016/j.ndteint.2016.08.004.

[11] J. Ma and P. Cawley, “Low-frequency pulse echo reflection of the fundamental shear horizontal mode from part-thickness elliptical defects in plates,” *J. Acoust. Soc. Am.*, vol. 127, no. 6, pp. 3485–3493, 2010, doi: 10.1121/1.3409446.

[12] P. Rajagopal and M. J. S. Lowe, “Short range scattering of the fundamental shear horizontal guided wave mode normally incident at a through-thickness crack in an isotropic plate,” *J. Acoust. Soc. Am.*, vol. 122, no. 3, pp. 1527–1538, 2007, doi: 10.1121/1.2764472.

[13] A. Pau and D. V. Achillopoulou, “Interaction of shear and Rayleigh-Lamb waves with notches and voids in plate waveguides,” *Materials (Basel).*, vol. 10, no. 7, 2017, doi: 10.3390/ma10070841.

[14] A. C. Kubrusly, J. P. von der Weid, and S. Dixon, “Experimental and numerical investigation of the interaction of the first four SH guided wave modes with symmetric and non-symmetric discontinuities in plates,” *NDT E Int.*, vol. 108, no. October, p. 102175, 2019, doi: 10.1016/j.ndteint.2019.102175.

[15] M. Ratassepp, M. J. S. Lowe, P. Cawley, and A. Klauson, “Scattering of the fundamental shear horizontal mode in a plate when incident at a through crack aligned in the propagation direction of the mode,” *J. Acoust. Soc. Am.*, vol. 124, no. 5, pp. 2873–2882, 2008, doi: 10.1121/1.2987426.

[16] A. C. Kubrusly, M. A. Freitas, J. P. von der Weid, and S. Dixon, “Interaction of SH guided waves with wall thinning,” *NDT E Int.*, vol. 101, pp. 94–103, 2019, doi: 10.1016/j.ndteint.2018.10.007.

© 2019 by ASME